DECLASSIFIED

UCRL 211

Cy 2/B

UNIVERSITY OF CALIFORNIA

Radiation Laboratory

TWO-WEEK LOAN COPY

This is a Library Circulating Copy which may be borrowed for two weeks. For a personal retention copy, call Tech. Info. Division, Ext. 5545

BERKELEY, CALIFORNIA

DISCLAIMER

This document was prepared as an account of work sponsored by the United States Government. While this document is believed to contain correct information, neither the United States Government nor any agency thereof, nor the Regents of the University of California, nor any of their employees, makes any warranty, express or implied, or assumes any legal responsibility for the accuracy, completeness, or usefulness of any information, apparatus, product, or process disclosed, or represents that its use would not infringe privately owned rights. Reference herein to any specific commercial product, process, or service by its trade name, trademark, manufacturer, or otherwise, does not necessarily constitute or imply its endorsement, recommendation, or favoring by the United States Government or any agency thereof, or the Regents of the University of California. The views and opinions of authors expressed herein do not necessarily state or reflect those of the United States Government or any agency thereof or the Regents of the University of California.

UNIVERSITY OF CALIFORNIA
Radiation Laboratory

DECLASSIFIED

SECRET

Cover Sheet
Do not remove

INDEX NO. UCRL-211
This document contains 8 pages
and 12 plates of figures.
This is copy 2 of 15 Series B

Issued to UCRL

CLASSIFICATION CHANGED BY AUTHORITY OF THE DECLASSIFICATION COMMITTEE

Classification

SECRET

Each person who receives this document must sign the cover sheet in the space below.

Route to	Noted by	Date	Route to	Noted by	Date
	Wilson	1/19/49			
M [illegible]	[illegible]	request			
	[illegible]	Dec 50			

DECLASSIFIED

UCRL-211

SECRET

CLASSIFICATION CANCELLED BY AUTHORITY OF THE DISTRICT ENGINEER BY THE DECLASSIFICATION COMMITTEE

UNIVERSITY OF CALIFORNIA

Radiation Laboratory

SECRET

Contract No. W-7405-eng-48

DECLASSIFIED

KINETIC ENERGY RELEASE IN FISSION OF U^{238}, U^{235}, Th^{232}, AND BI^{209} BY HIGH ENERGY NEUTRONS

J. Jungerman and S. C. Wright

November 11, 1948

CLASSIFICATION CANCELLED
BY AUTHORITY OF THE DECLASSIFICATION BRANCH USAEC ON 12-23-58
DATE
By B. Robert
SIGNATURE OF THE PERSON MAKING THE CHANGE

Berkeley, California

DECLASSIFIED

SECRET

KINETIC ENERGY RELEASE IN FISSION OF U^{238}, U^{235}, Th^{232} AND Bi^{209} BY HIGH ENERGY NEUTRONS

CLASSIFICATION CANCELLED BY AUTHORITY OF THE DECLASSIFICATION COMMITTEE

J. Jungerman and S. C. Wright

Radiation Laboratory, Department of Physics
University of California, Berkeley, California

November 11, 1948

SECRET

Abstract

The ionization produced by single fission fragments was observed in an ionization chamber using electron collection. Employing 90 Mev neutrons one energy group only is observed with the most probably fragment energy centrally located in contrast to the double-peaked curve obtained with thermal neutron fission. The most probable single fragment energy is for U^{238}, 78 Mev; U^{235}, 81 Mev; Th^{232}, 81 Mev; Bi^{209}, 74 Mev. The mean energy of the fragments is for U^{238}, 75 Mev; U^{235}, 82 Mev; Th^{232}, 80 Mev; and Bi^{209}, 71 Mev. It should be emphasized that this report is preliminary and that the experiment is still in progress.

DECLASSIFIED

SECRET DECLASSIFIED

SECRET

Kinetic Energy Release in Fission of U^{238}, U^{235}, Th^{232} and Bi^{209} By High Energy Neutrons

J. Jungerman and S. C. Wright

Radiation Laboratory, Department of Physics
University of California, Berkeley, California

CLASSIFICATION CHANGED BY AUTHORITY OF THE DISTRICT ENGINEER BY THE DECLASSIFICATION COMMITTEE

November 11, 1948

Introduction:

The kinetic energy release occuring in low energy neutron fission has been studied by Jentschke[1], Flammerfeld et al[2], Brolley[3], Deutsch and Ramsey[4], and Fowler and Rosen[5]. The results of these experiments show the kinetic energy of single fragments to be divided into two distinct groups. The energy distribution was consistent with the mass distribution of the fragments known from chemical evidence and the assumption that the kinetic energy observed was derived only from the coulomb repulsion of two charged fragments[4]. The object of the experiment reported here was to investigate the distribution of kinetic energy of single fragments produced by 90 Mev neutron fission and the influence of the increased excitation on the mean fragment energy. To this aim the kinetic energy of single fragments was measured by the use of a grid ionization chamber, a linear amplifier, and a camera for photographically recording pulse heights on an oscilloscope.

Experimental:

Fig. 1 shows a diagram of the ionization chamber employed. Each target plate had a foil spot welded to its surface covered with the element under investigation. The foils in the case of uranium or thorium were prepared by painting a solution of the nitrate on 1 mil aluminum and baking at 500 C. until the oxide was formed[6]. The amount of material never exceeded 3×10^{-5} gm./cm^2. Foils surfaced with 5×10^{-5} gms/cm^2 of bismuth were prepared by raporation of the metal on 1 mil aluminum.

The grids consisted of 3 mil nichrome wire 50 mils apart. The electrodes were so arranged that the distance between the target plate and grid was greater than the range of

DECLASSIFIED
SECRET

CLASSIFICATION CANCELLED BY AUTHORITY
OF THE DISTRICT ENGINEER
BY THE DECLASSIFICATION COMMITTEE

fragments. The voltages provided a small tunnel effect and were sufficiently high to insure saturation of the fission pulses[4]. The chamber was filled with pure argon at a pressure of 160 cm of Hg.

The chamber walls and electrodes were made as thin as practicable in order to reduce the background ionization due to charged particles produced by the neutron beam. The neutron beam entered through a .002 stainless steel window, traversed a .001 aluminum foil with the sample on it, the grid, and finally a .0005 aluminum foil collection plate. It then passed on through a similar unit of two plates and a grid. There were 4 such units in all. The last usually contained a sample of U^{235} for calibration purposes.

The electronic circuit is shown schematically in Fig. 2. This arrangement was employed in order to discriminate against pulses caused by high energy neutron reactions in the argon and chamber plates along the path of the neutron beam. By the use of a delay line and a five microseconds sweep it was possible to see the start of the trace, the pulse rise, and the first part of the decay. Fig. 3 shows the form of a typical pulse. The distance x in the figure was taken to be the pulse height. Any pulse whose form differed from that of figure 3 was rejected. Figure 4 is an exaggerated example of such a rejected pulse. These unsatisfactory pulses were assumed to be due to a combination of ionization produced by neutron reactions in the electrodes and gas and fission fragment ionization. A discriminator on the intensifier input was used to prevent a prohibitive number of low energy pulses from being recorded. Fast rise time stabilized amplifiers were used. The fission pulses had a rise time of 1.5 microseconds and decayed to 1/e in 10 microseconds. A fast rise time pulse generator connected when required to the grid of the chamber checked the linearity and amplification of the equipment on the different bombardments. Calibration pulses from the pulse generator were used before and after each run.

The pulses on the Dumont 248 oscilloscope were photographed with a camera using continuously moving 35 mm. Super XX film. All pulse heights were measured on the same microfilm viewer.

The usual experimental arrangement in the ionization chamber was to have a sample

DECLASSIFIED

SECRET

of U^{235} on plate A and samples of the substance under investigation on plates B. (See Fig. 1). Immediately before or after a cyclotron run a fission fragment energy distribution was made with slow neutrons on U^{235} using the same chamber gas and the same setting of the amplifier and oscilloscope. The only change made was in the position of the apparatus. This procedure permitted a comparison of the fast neutron experimental results with the U^{235} (slow neutron fission) fragment energy distribution, and therefore provided a check on the resolution of the chamber and the absolute energy scale. Since the cyclotron magnetic field was different at the bombardment and calibration positions a check of the effect of the effect of position on the amplification of the apparatus was made by making slow neutron runs at both locations. The pulse height average was found to be 3 percent higher at the bombardment position. This factor has been included in the energy scale calculation.

The high energy neutrons used in these experiments were formed by bombardment of a 3/8" Be target with 190 Mev deuterons. Ra-Be enclosed in paraffin provided a thermal neutron source.

Results:

Figures 5, 6, 7, and 8 show the actual histograms of the fragment energies of U^{238}, U^{235}, Th^{232}, and Bi^{209}. Figure 9 shows a typical slow neutron calibration histogram. Figure 10 shows the probable distribution corresponding to these histograms. Cyclotron runs made with an aluminum blank of the same thickness, .001", as that supporting the sample showed that the number of pulses corresponding to fission fragments of 40 Mev. and above were negligible. It is found that the mean fragment energy is 75 Mev. for U^{238}, 82 Mev for U^{235}, 80 Mev for Th^{232}, 71 Mev for Bi^{209}. The energy spread at one half maximum is 44 Mev for U^{238}, 33 Mev for U^{235}, 41 Mev for Th^{232}, 25 Mev for Bi^{209}. The energy scale for the figures was obtained by comparison of the slow neutron calibration curve for each run with the curve of Deutsch and Ramsey. This was checked within the experimental error by measuring the pulses produced in our apparatus by the alpha particles of U^{234}. Tentative results have been obtained for the distributions using 45 Mev neutrons and they will be reported in a later paper.

SECRET

cussion:

The foregoing assumes that the number of ion pairs is proportional to the energy of the fission fragments producing them.

If the fission is assumed to be binary, the mode of fission induced by 90 Mev neutrons that gives equal kinetic energies to the fragments is the most probable one in contrast to the results of thermal neutron fission. The mean kinetic energy of the fragments is, in the case of U^{235}, only 2 Mev higher than that from fission induced by slow neutrons. The kinetic energy of the incident neutron must therefore be accounted for by some other mechanism than appearance in the kinetic energy of the fission fragments.

Goekermann and Perlman[7] have investigated fission products forms from bismuth by 200 Mev deuterons. They find that the mass number distribution has a maximum at about 100 mass units. This indicates a loss of approximately 10 neutrons from the compound nucleus before fission takes place.

The following mechanism is tentatively suggested for the fission process caused by high energy neutrons. See Fig. 11. The compound nucleus Z^{A+1^*} formed from the nucleus Z^A by capture of a high energy neutron evaporates J neutrons until its energy A above the ground level is less than the binding energy C of a neutron to the nucleus Z^{A+1-J^*}. Fission may be expected to have a threshhold at some energy B above the ground level. If the level A is above B, fission may occur; if it is below B only gamma emission is possible. Thus in general when the level A is reached, two processes, gamma radiation and fission are important for the removal of the remaining excitation. Their mean lives are long compared with that for neutron emission where the latter is energetically possible and they will be unimportant during the initial evaporation process. The relative probabilities of A being above or below the fission threshhold B should be proportional to the number of levels available in the two regions. According to the above picture fission should occur in a relatively unexcited compound nucleus competition with gamma emission and therefore exhibit a cross section for fission less than the geometrical with fluctuations from element to element. This is in agreement with the following. Recent measurements by Jungerman, Kelly, Wiegand, and Wright give the absolute

fission cross section for 90 Mev neutrons on uranium and thorium to be 1.4 barns and .97 barns respectively. In each case the cross section is less than one half the geometric cross section and also the two values differ considerably.

In the high energy neutron fission of U^{235} the mean kinetic energy of the fragments is only slightly higher than that of the thermal neutron fission fragments. For Bi^{209} the mean fragment energy is .87 times the latter. It was pointed out in the introduction that the energy distribution of the fragments in thermal neutron fission is consistent with their known mass distribution under the assumption that the kinetic energy observed is derived from the coulomb repulsion of two charged fragments. Since it has been suggested above that in high energy neutron fission the actual division of the nucleus only occurs in a relatively unexcited state, in fact of the same order of excitation as in the thermal neutron case, the high energy case should agree with a similar treatment. This can be easily checked for symmetrical fission with the crude model of Fig. 12. At the moment of separation the two fragments are assumed spherical in shape with a uniform distribution of charge and radii $R = r_0 \times A^{1/3}$ where A is the mass number of the fragment and r_0 is a constant. Also the charge of the fragments is assumed proportional to their mass. Under these conditions the coulomb potential energy E_c at the moment of separation will be

$$E_c = \frac{(Z^1 \; Z^{11})\, e^2}{r_0 \, (A^{1\;1/3} + A^{11\;1/3})}$$

and for symmetrical fission: $E_{c,s} = \dfrac{(Z^1 \, e)^2}{2 \, r_0 \, (A^1)^{1/3}} \quad \dfrac{(Z/2 \, e)^2}{2 \, r_0 \left(\dfrac{A - J + 1}{2}\right)^{1/3}}$

Comparison of $E_{c,s}$ for 90 Mev neutrons on Bi^{209} and placing J equal to 10 with $E_{c,s}$ for thermal neutrons on U^{235} gives the ratio .86 which agrees well with the experimental value quoted above.

Acknowledgments:

We wish to thank C. Wiegand for some electronic equipment and for many valuable suggestions during the course of this work. We are deeply indebted to Professor E. Segrè for suggesting this problem and for many stimulating discussions throughout the course of the

stigation. Thanks are also due the 184" cyclotron crew for valuable cooperation.

References:

1. Zeit. fur Physik, 120, 165 (1943).

2. Zeit. fur Physik, 120, 450 (1943).

3. CN 1840

4. LADC 257

5. Phys. Rev., 72, 926 (1947).

6. T. Jorgenson, MDDC 467.

7. Phys. Rev. 73, 1127 (1948).

RLID/hw
11-12-48

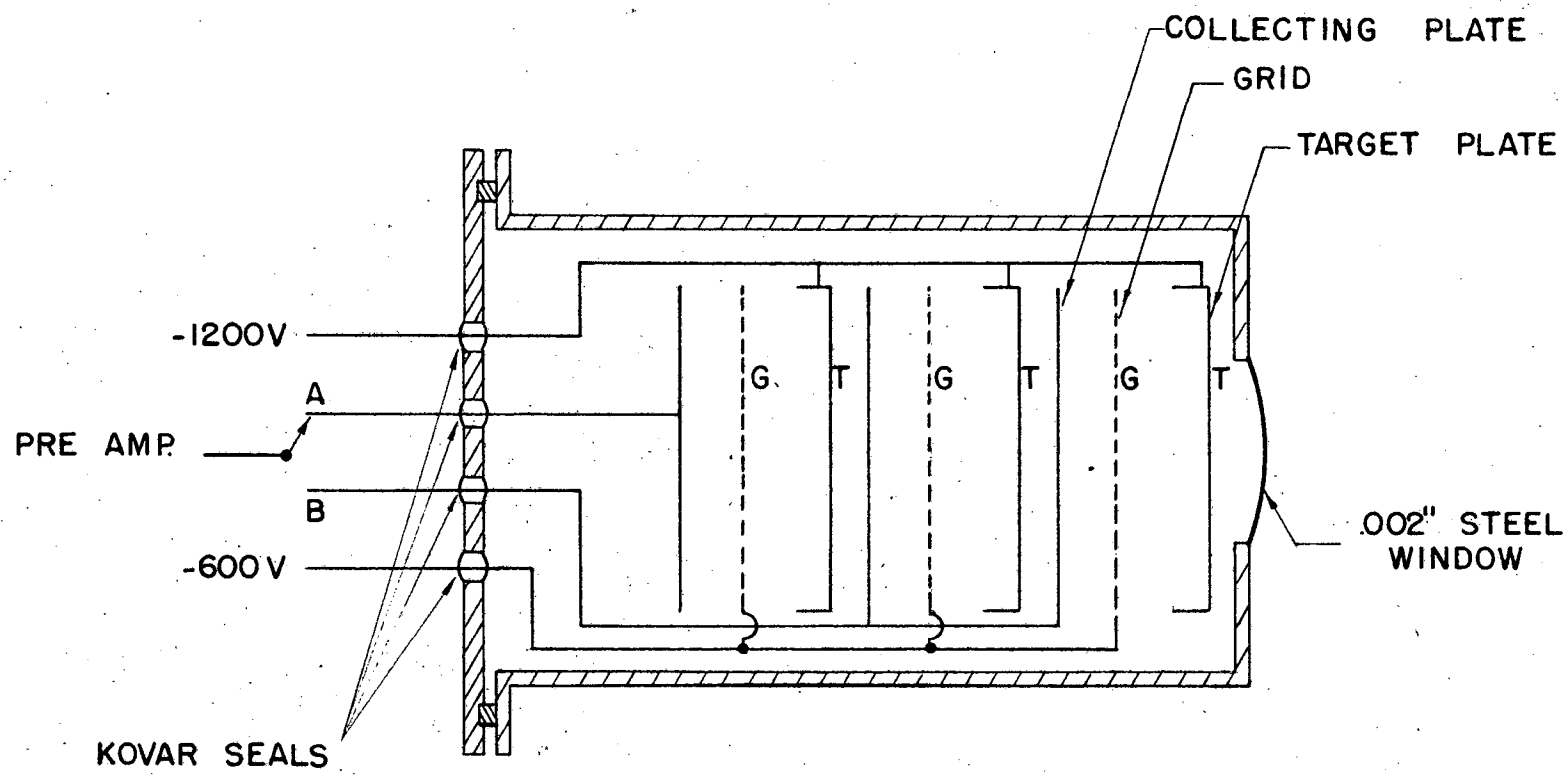
COLLECTING PLATE
GRID
TARGET PLATE
-1200V
A
PRE AMP.
B
-600V
G
T
G
T
G
T
.002" STEEL WINDOW
KOVAR SEALS

FIG.1

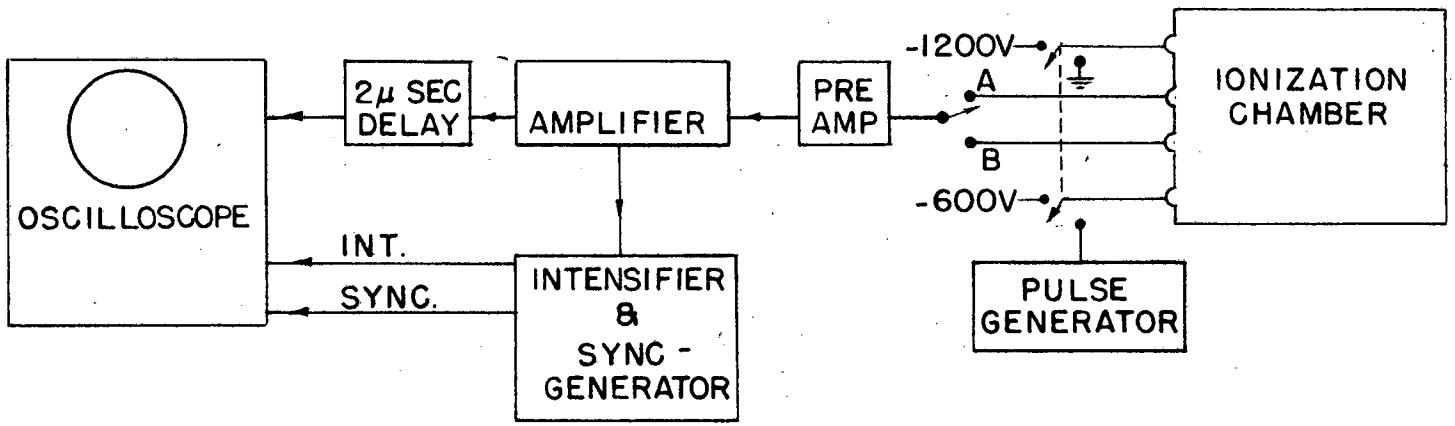
OSCILLOSCOPE
2μ SEC DELAY
AMPLIFIER
PRE AMP
-1200V
A
B
-600V
IONIZATION CHAMBER
INT.
SYNC.
INTENSIFIER & SYNC - GENERATOR
PULSE GENERATOR

FIG. 2
13108

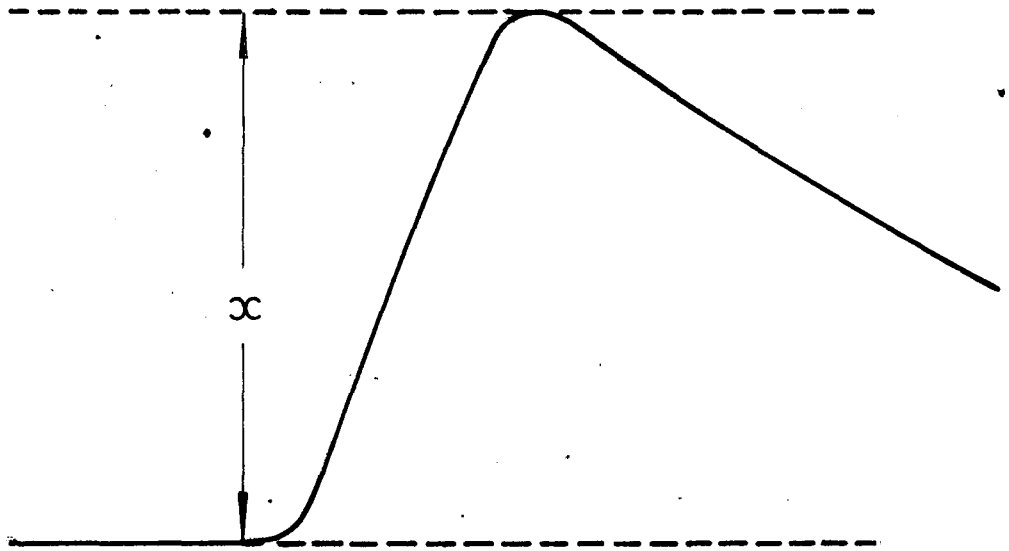

FIG. 3
13109

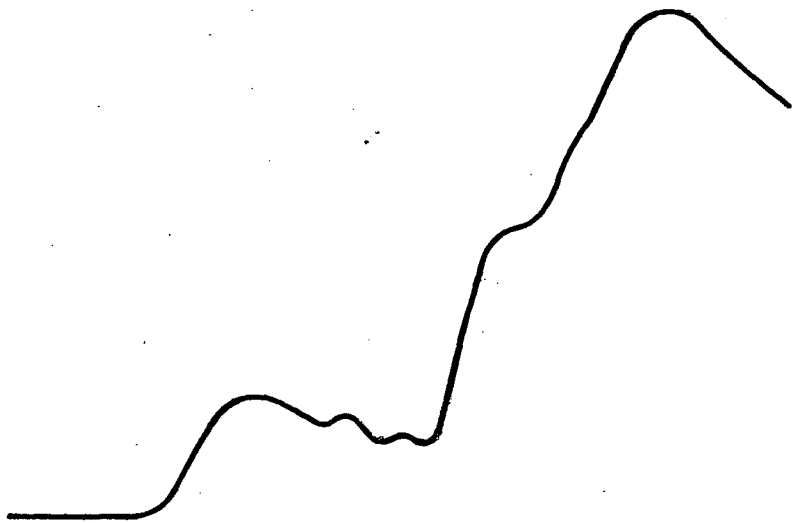

FIG. 4

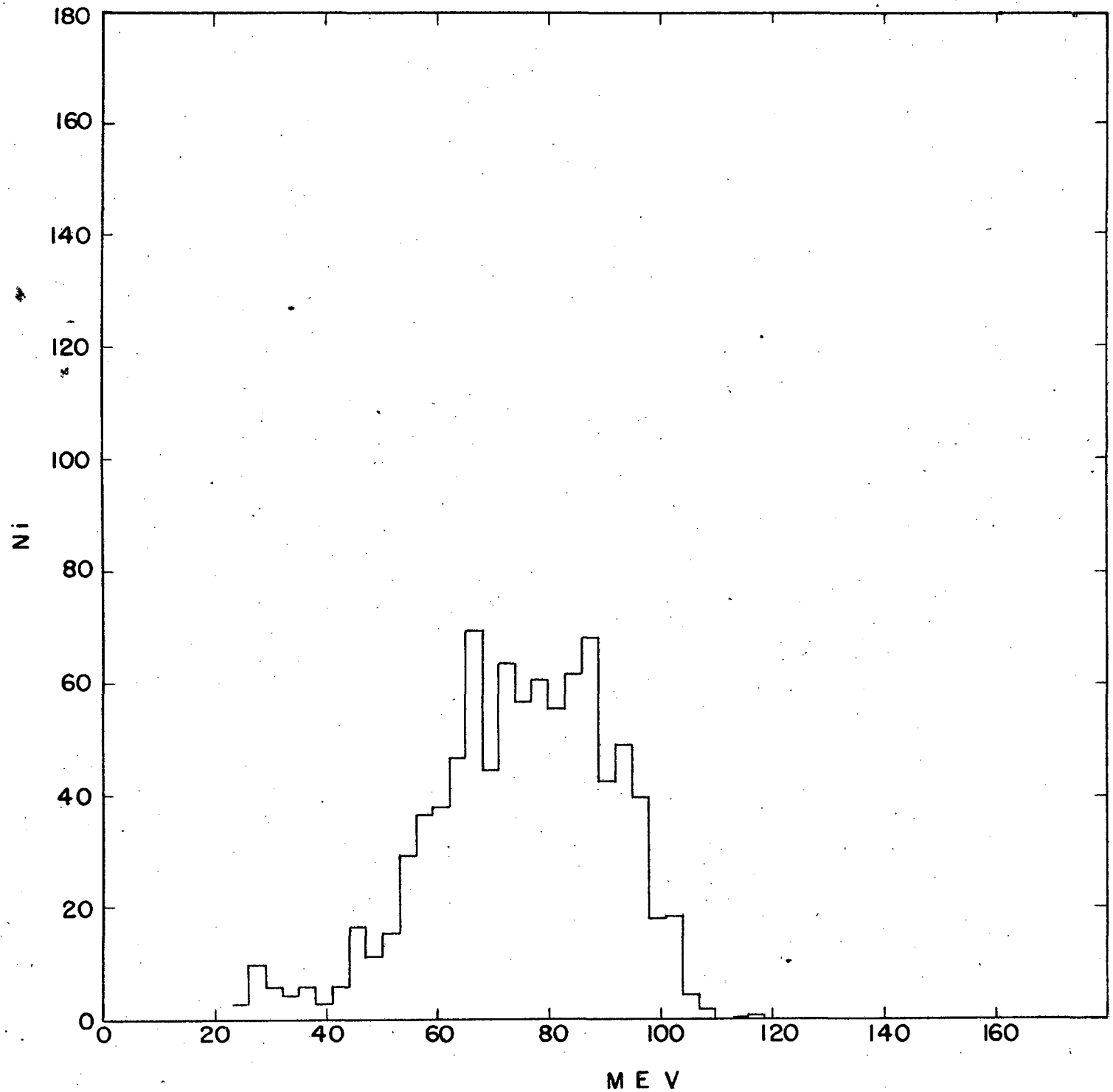
180
160
140
120
100
80
60
40
20
0
Ni
0
20
40
60
80
100
120
140
160
M E V

FIG. 5
1311

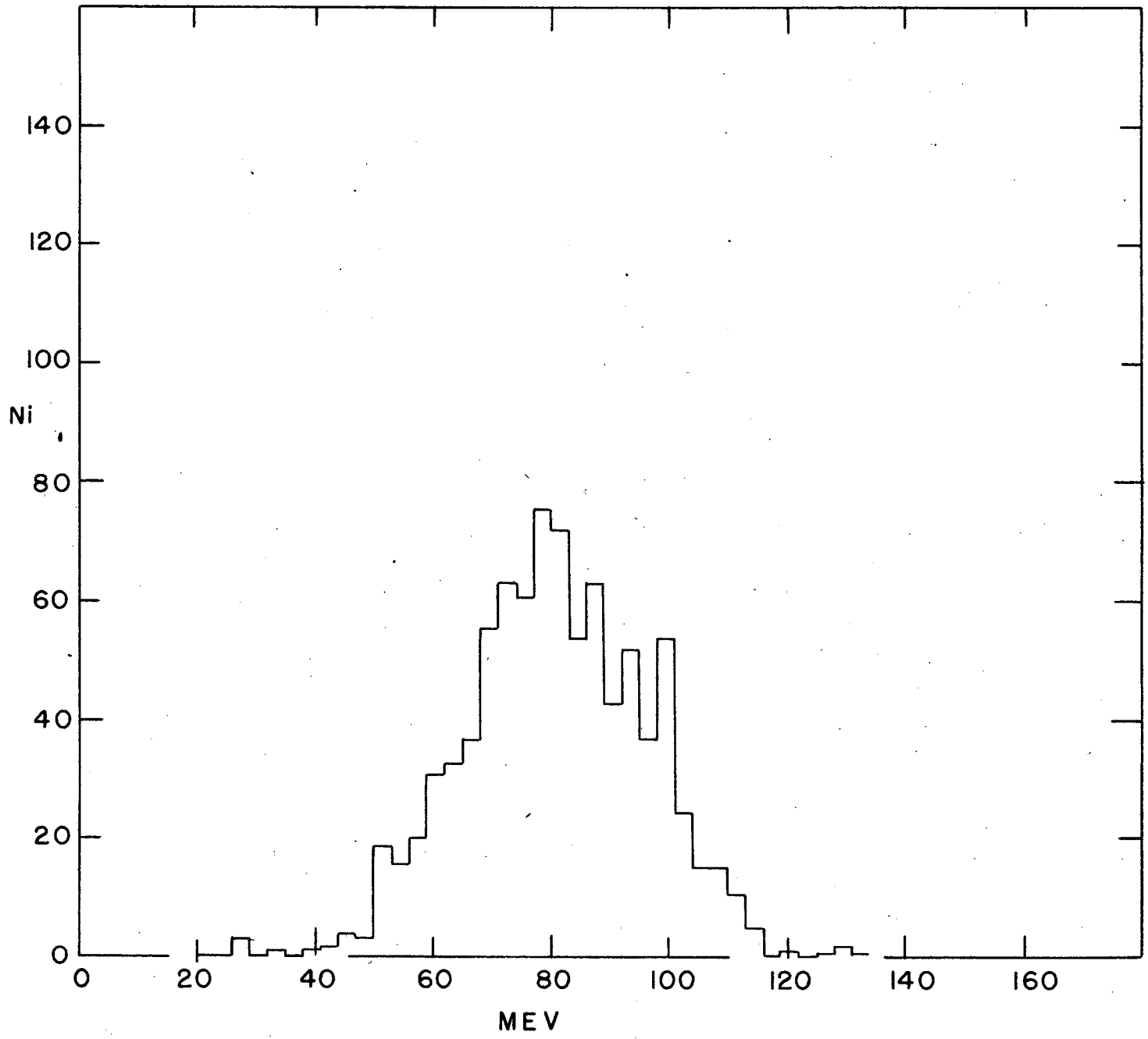

FIG. 6
13114-1

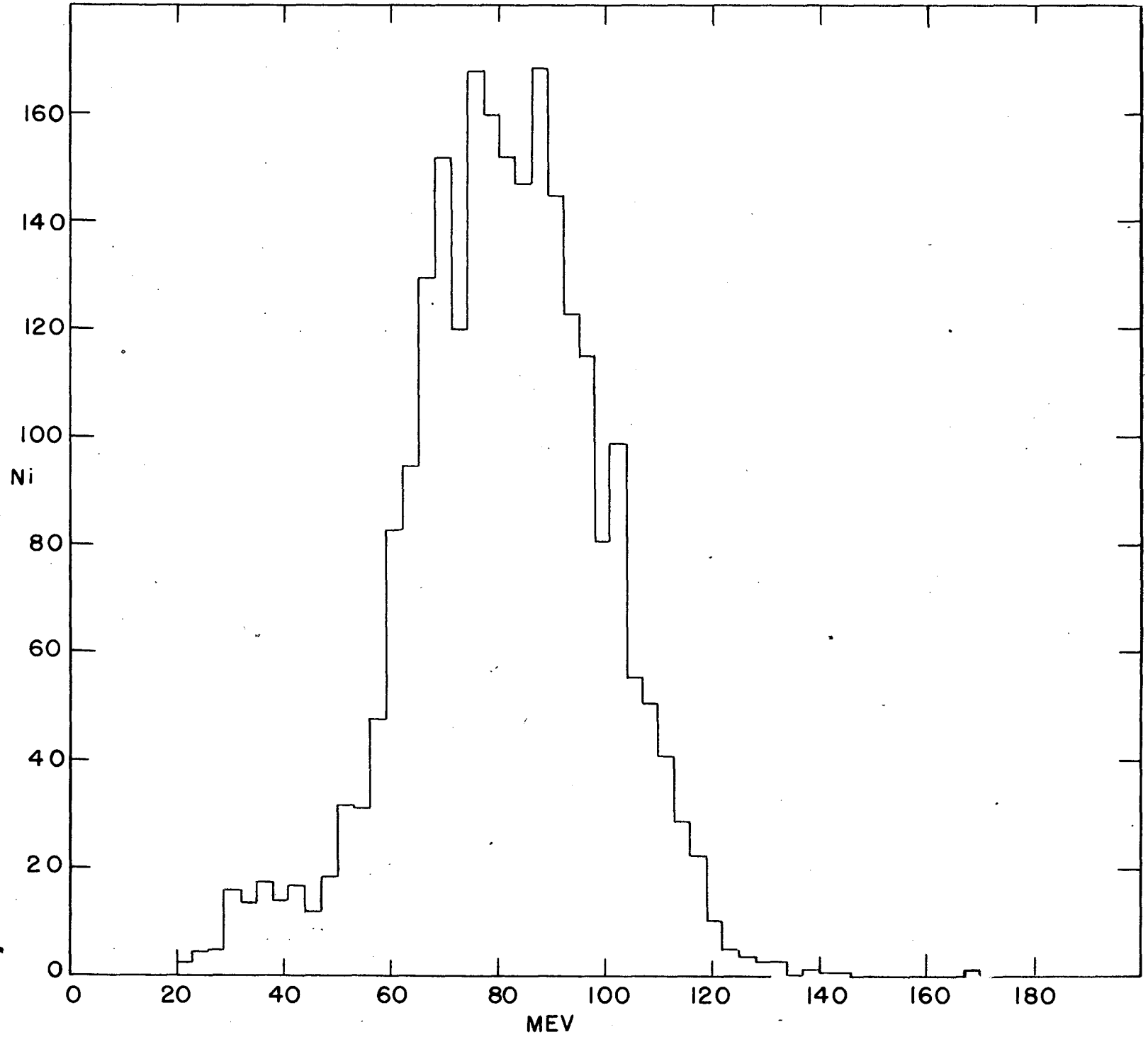
160
140
120
100
Ni
80
60
40
20
0
0
20
40
60
80
100
120
140
160
180
MEV

FIG.

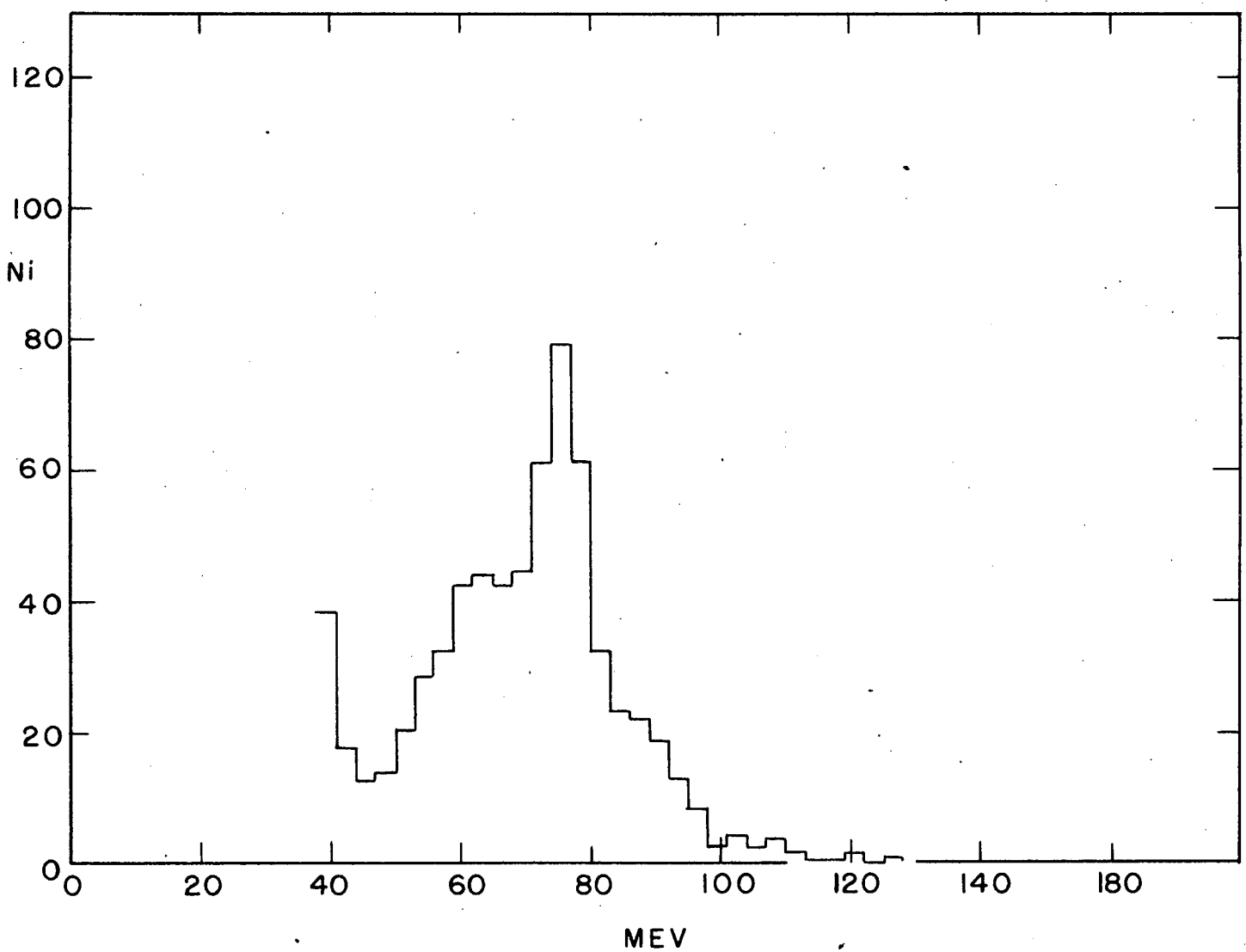

FIG 8
13116-

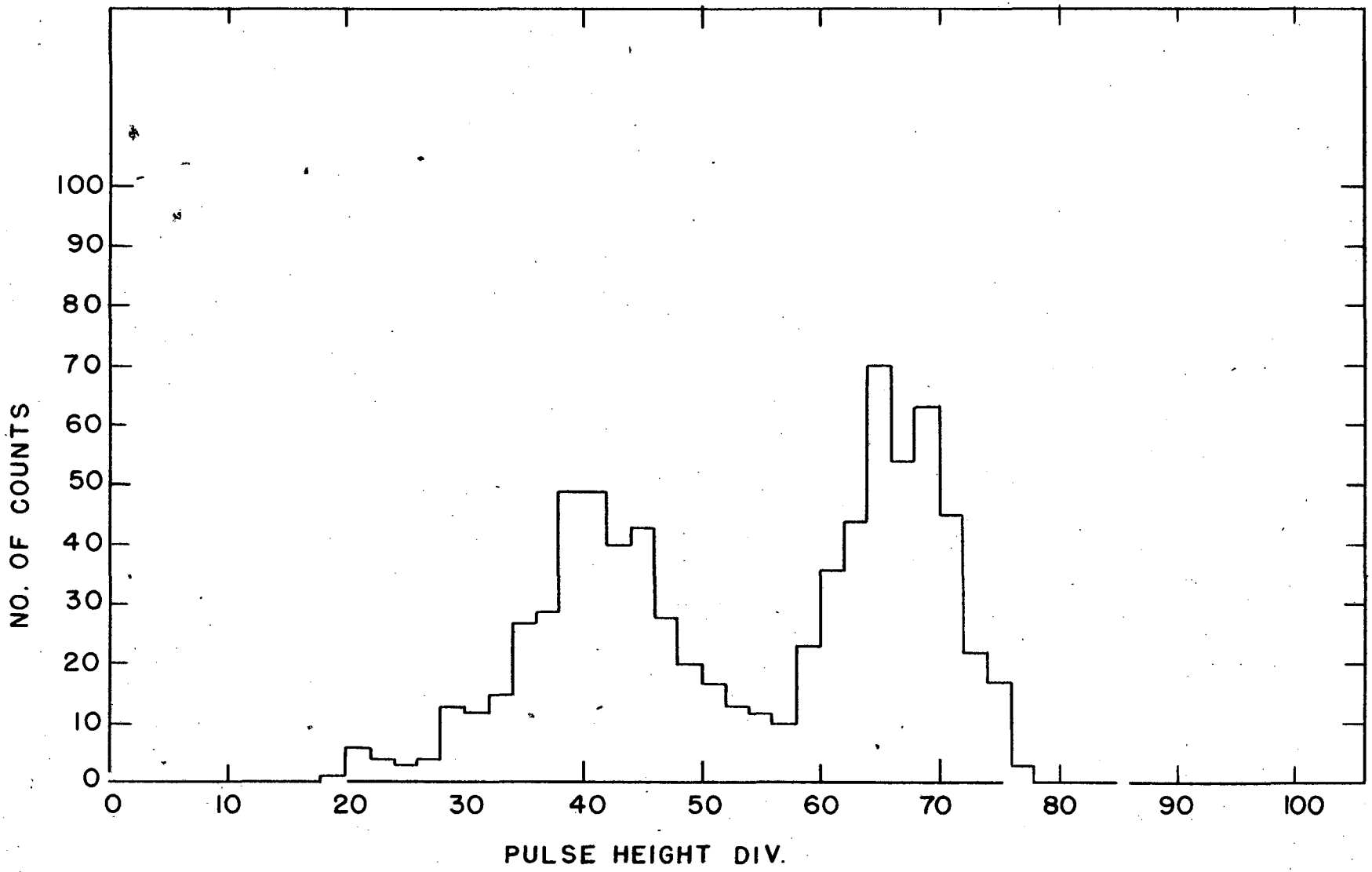

FIG. 9

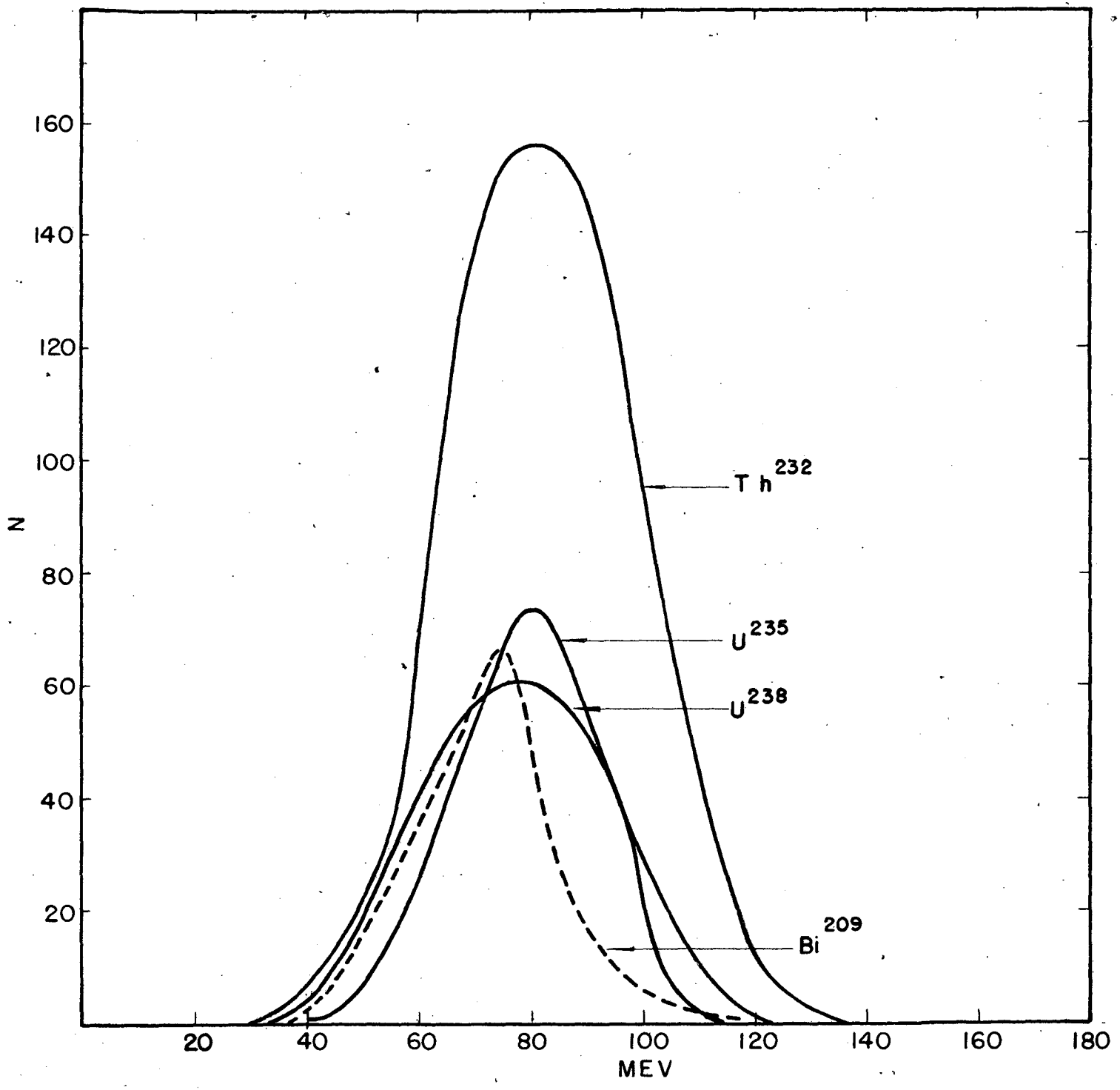
160
140
120
100
80
60
40
20
N
20
40
60
80
100
120
140
160
180
MEV
Th 232
U 235
U 238
Bi 209

FIG. 10

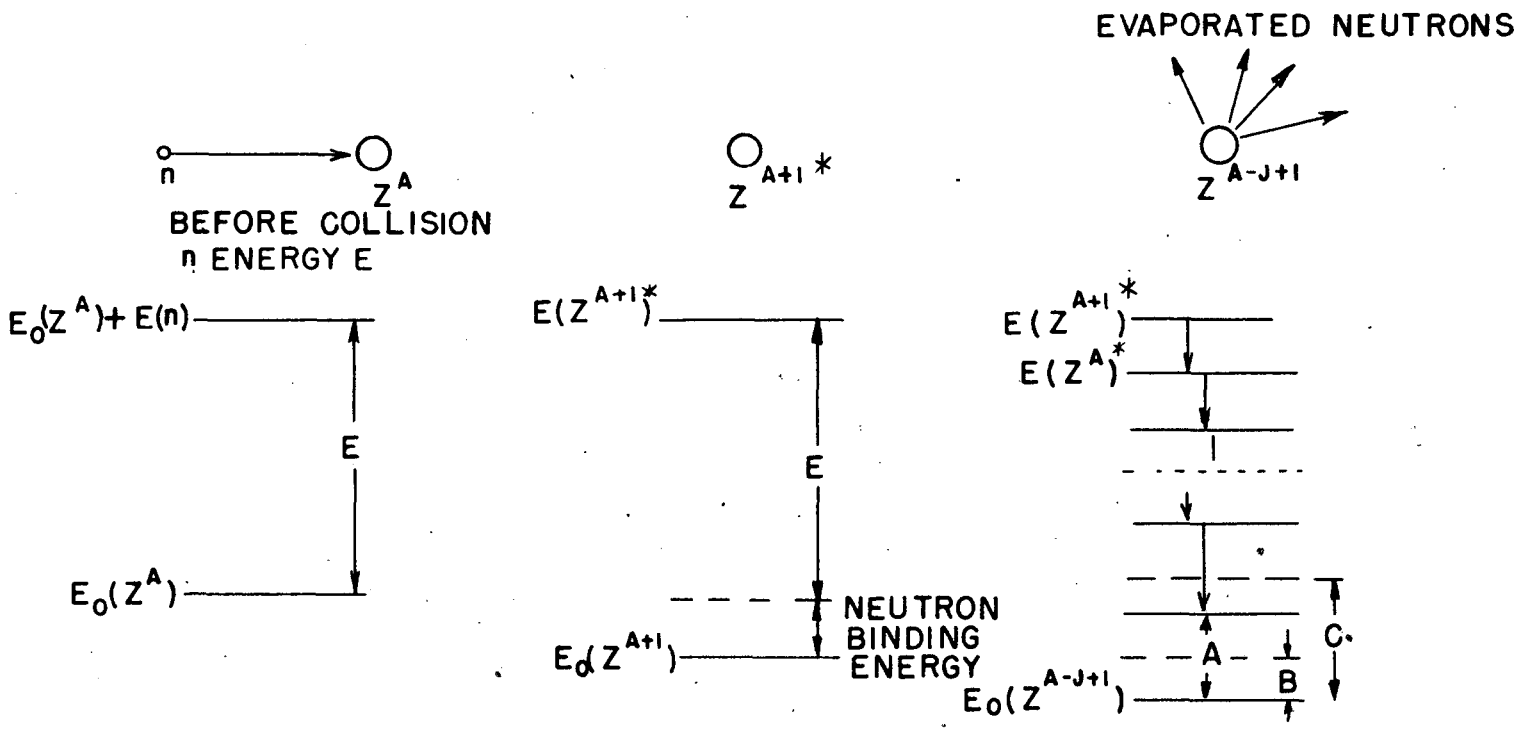
EVAPORATED NEUTRONS
n
Z^{A}
BEFORE COLLISION
n ENERGY E
Z^{A+1*}
Z^{A-J+1}
$E_0(Z^A) + E(n)$
E
$E_0(Z^A)$
$E(Z^{A+1*})$
E
NEUTRON
BINDING
ENERGY
$E_0(Z^{A+1})$
$E(Z^{A+1*})$
$E(Z^{A*})$
A
B
C
$E_0(Z^{A-J+1})$

FIG. 1
13118-

DECLASSIFIED

FIGURE CAPTIONS

Fig. 1. Ionization chamber. Electrode supports are not shown.

Fig. 2. Electronic circuit.

Fig. 3. Typical Pulse Form.

Fig. 4. Unsatisfactory pulse.

Fig. 5. Single fragment energy distribution. 90 Mev "n" on U^{238}.

Fig. 6. Single fragment energy distribution. 90 Mev "n" on U^{235}.

Fig. 7. Single Fragment energy distribution. 90 Mev "n" on Th.

Fig. 8. Single fragment energy distribution. 90 Mev "n" on Bi.

Fig. 9. Typical slow neutron calibration histogram.

Fig. 10. Most probable single fragment energy distribution. 90 Mev "n" on U^{238}, U^{235}, Bi^{209}, and Th^{232}.

Fig. 11. Proposed energy level diagram for high energy neutron fission.

Fig. 12. Model for fission fragments at the moment of separation.
Assumed process:

$$Z^{A} + n \longrightarrow Z^{1A^{1}} + Z^{11A^{11}} + J(n)$$

$$A = A^{1} + A^{11} + (J-1)n$$

$$\frac{Z^{1}}{Z^{11}} = \frac{A^{1}}{A^{11}}$$

DECLASSIFIED

DECLASSIFIED

SECRET

RESTRICTED

CLASSIFICATION CANCELLED BY AUTHORITY
OF THE DISTRICT ENGINEER
BY THE DECLASSIFICATION COMMITTEE

DECLASSIFIED

[redacted]

DECLASSIFIED

[redacted]